# Strong Exciton–Photon Coupling and Lasing Behavior in All-Inorganic CsPbBr3 Micro/Nanowire Fabry-Pérot Cavity

# Strong Exciton-Photon Coupling and lasing behavior in All-Inorganic $CsPbBr_3$ Micro/nanowire Fabry-Pérot cavity

*Wenna Du,[†,#] Shuai Zhang,[†,‡,#] Jia Shi [†,‡] Jie Chen,[†,‡] Zhiyong Wu,[†] Yang Mi,[†] Zhixiong Liu,[⊥] Yuanzheng Li,[†] Xinyu Sui,[†,‡] Rui Wang,[†] Xiaohui Qiu,[†] Tom Wu,[⊥] Yunfeng Xiao,[ℓ,*] Qing Zhang,[§,*] and Xinfeng Liu[†,‡,*]*

[†]Division of Nanophotonics, CAS Key Laboratory of Standardization and Measurement for Nanotechnology, CAS Center for Excellence in Nanoscience, National Center for Nanoscience and Technology, Beijing 100190, P. R. China

[‡]University of Chinese Academy of Sciences, Beijing 100049, P.R. China

[§]Department of Materials Science and Engineering, College of Engineering, Research Center for Wide Band Semiconductor, Peking University, Beijing 100871, P. R. China

[⊥]Laboratory of Nano Oxides for Sustainable Energy, Material Science and Engineering (MSE), King Abdullah University of Science & Technology (KAUST), Thuwal, 23955-6900, Saudi Arabia

[ℓ]State Key Laboratory for Mesoscopic Physics, Collaborative Innovation Center of Quantum Matter, School of Physics, Peking University, Beijing
100871, China

[#]Wenna Du and Shuai Zhang contributed equally to this work.

*Email address: liuxf@nanoctr.cn, q_zhang@pku.edu.cn and yfxiao@pku.edu.cn

**ABSTRACT**

All-inorganic perovskite micro/nanowire materials hold great promises as nanoscale coherent light source due to their superior optical and electronic properties. The coupling strength between exciton and photon in this system is important for their optical application, however, is rarely studied. In this work, we demonstrated the strong coupling of exciton-photon and polariton lasing in high quality $CsPbBr_3$ micro/nanowires synthesized by a CVD method. By exploring spatial resolved PL spectra of $CsPbBr_3$ cavity, we observed mode volume dependent coupling strength with a vacuum Rabi splitting up to 656 meV, as well as significant increase in group index. Moreover, low threshold polariton lasing was achieved at room temperature within strong coupling regime; the polariton characteristic is confirmed by comparing lasing spectra with waveguided output spectra and the dramatically reduced lasing threshold. Our present results provide new avenues to achieve high coupling strengths potentially enabling application of exciting phenomena such as Bose-Einstein condensation of polaritons, efficient light-emitting diodes and lasers.

**Keywords**: $CsPbBr_3$ Nanowires, Exciton-photon Coupling, Microcavity, Waveguide, Polariton lasing

Lead halide perovskites have recently become a rapidly growing research field due to their unprecedented success in next-generation solar cells.[1-5] The power conversion of solution-processed $CH_3NH_3PbX_3$ (X= Cl, Br, I) perovskite solar cells has reached 22.1% within few years.[6] Meanwhile, as a direct bandgap semiconductor, perovskites are also promising candidates with great potential in photonic sources due to their high optical gain, ease of bandgap engineering, large absorption coefficient, and low defect state density.[1-4, 7-11] Recently, all-inorganic lead halide perovskites ($CsPbX_3$, X= Cl, Br, I) have attracted much attention due to long-term thermal and hydrolysis stabilities comparing with their hybrid organic–inorganic counterparts, with excellent optical properties at the same time.[9, 12-14] For instance, Eaton *et al*. reported ultrastable pure-inorganic $CsPbBr_3$ perovskite-nanowire lasers that worked in ambient and vacuum conditions.[15] The lasing behavior lasted even after $10^9$ excitation cycles with a low threshold of 5 μJ/cm$^2$ and an excellent lasing spectra coherence of $\approx$0.5 nm. All-inorganic lead halide perovskites grown by an epitaxy-free vapor phase technique exhibit excellent optical gain properties with large exciton binding energy and oscillator strength.[16] Multicolor lasing is achieved with low threshold (~2 μJ/cm$^2$) and high spectra coherence (~0.14-0.15 nm), and better optical stability under high laser flux illumination compared with hybrid perovskites. Very recently, strong exciton-photon interaction in $CsPbBr_3$ perovskites has been exhibited and a polariton related lasing are proposed from these nanowires by Park and coworkers.[17] Meantime, room-temperature polariton lasing based on the all-inorganic $CsPbCl_3$ nanoplatelet microcavity has also been reported by Su *et al.* lately.[18] These demonstrations

mentioned above have motivated us to explore the mechanism of strong light-matter coupling and the relationship between coupling strength and lasing threshold in inorganic lead halide perovskite samples.

Exciton-polaritons,[19-21] bosonic quasi-particles resulting from the strong coupling between electron-hole pairs (excitons) and photons confined in an optical microcavity, are fundamental to many exciting phenomena.[22-27] The exciton-polariton coupling strength in an optical microcavity is expressed as the Rabi splitting energy, $2\hbar g \propto 2\hbar\sqrt{n * f/V_m}$, [28-29] with $\hbar$ reduced Planck constant, $n$ the number of oscillators, $f$ their oscillator strength, and $V_m$ the mode volume. Coupling between exciton resonance and photon is enhanced in micro/nanowire cavity due to enhancement of oscillator strength and coupling with small mode volume low-loss optical cavities.[28, 30-33] Moreover, by integrating advantages of perovskites and one dimensional material, such as ultra-compact physical sizes, highly localized coherent output, and efficient waveguide, Zhu *et al.* reported the first demonstration of perovskite nanowire lasers.[11] After that, ultra-stable $CsPbX_3$ micro/nanowires laser have also been demonstrated with low thresholds and excellent lasing spectra coherence.[34] Therefore, all-inorganic perovskite nanowires are ideal systems to study the light−matter interactions. Park *et al.* found the uneven mode spacing in pulsed lasing from $CsPbBr_3$ nanowires, suggesting the possibility of strong light-matter interactions.[17] However, intrinsic mechanism accounting for strong coupling strength occurred in $CsPbX_3$ was not yet well studied. The nature of waveguiding in nanowires is different from its bulk counterpart and light−matter interactions are expected to be strong in nanowires

because the extent of coupling between the photon (light) and the exciton (matter) is strengthened by the decrease in the mode volume and the high oscillator strength in nanowires. It will be an ideal platform to investigate the fundamental properties of exciton-polariton and to accomplish scalable and high performance polariton lasing operated at room temperature. Very recently, we observed clear anticrossing feature of strong exciton–photon coupling in inorganic–organic hybrid perovskite nanowires and the coupling strength could be weakened because of carrier screening effect with increasing pump fluence.[35] At the same time, continuous wavelength (CW) lasing from polariton modes condensed in the bottleneck region of $CsPbBr_3$ nanowires is realized by Zhu's research group,[36] which may open the door to model systems for polaritonics in the strong-coupling regime.

In this study, we realized size-tunable light-matter interactions and polariton lasing in the one-dimensional cavity using all-inorganic $CsPbBr_3$ perovskite micro/nanowires synthesized by a chemical vapor deposition (CVD) method. We measured the spatial resolved PL spectra of the $CsPbBr_3$ nanowires waveguide with different mode volume and analyzed the Fabry-Pérot modes that form along the length direction of the nanowires. Strong exciton-polariton coupling strengths characterized by a vacuum Rabi splitting of up to 656 meV, as well as a significant increase in group index have been achieved. More significantly, by comparing the lasing spectra with the guided PL spectra, it is confirmed that the modes of the lasing spectra at room temperature with low threshold belong to the polariton lasing. Our current results suggest considerable promise of inorganic lead halide perovskite

toward low-cost, high-performance room-temperature polariton devices.

## RESULTS AND DISCUSSION

Strong exciton-photon coupling can commonly be observed in optical microcavities, especially a micro/nanowire Fabry-Pérot cavity with small mode volume and nature of waveguiding. Photons propagate along the axial direction and oscillate between the two end-facets of the nanowires. If the electromagnetic wave in this optical cavity is nearly resonant with interband exciton transition, then one cannot make the distinction between them and then cavity polaritons formed as shown in **Figure 1a**. Instead, the energy oscillates between trapped photons and exciton until dissipation of this coherent state.[37] Here, we study the exciton-photon coupling in the material system of $CsPbBr_3$ micro/nanowires with large exciton binding energy [16, 38] and high intrinsic exciton oscillator strength.[39] They were grown on $SiO_2$/Si substrates using a CVD method. A detailed description of the micro/nanowire growth method and characterization could be found in the *Supporting Information* **Note1**. The $CsPbBr_3$ nanowires crystallized in the cubic phase [13, 16, 34] are featured with a well-defined tri-prism shape laying on the $SiO_2$ substrate as the representative scanning electron microscopy (SEM) shows (in **Figure 1b**), identical to the previous works.[34, 40]. Statistical results from SEM and Atomic force microscopy (AFM) (*Supporting Information,* **Figure S1 –S3**) demonstrate $CsPbBr_3$ nanowires with a highly smooth surface and an ideal size region for confining photonic mode in the nanowires and spatial resolved measurement. The cubic crystal structure and the $CsPbBr_3$ phase are

affirmed by the X-ray diffraction pattern and energy-dispersive X-ray spectroscopy (see *Supporting Information,* **Figure S4**). The optical performance of the $CsPbBr_3$ nanowires exhibited in **Figure S5** presents that the PL from single $CsPbBr_3$ perovskite nanowire is centered at ~531 nm (2.34 eV) similar to previous reported[41-44]. While a full width at half maximum (FWHM) of 15 nm (66 meV) is smaller than that of highly luminescent $CsPbBr_3$ CQDs (~12.0–42.0 nm) and $CsPbBr_3$ nanowires synthesized by solution method at room temperature, which suggests the high quality and good optical/excitonic properties of as-grown nanowires.[13, 15]

To probe the waveguide modes and polaritonic effects in $CsPbBr_3$ nanowires, we conducted the spatially resolved PL measurement with the nanowires as schematically shown in **Figure 1c**. Light guiding of PL signals is commonly observed in $CsPbBr_3$ nanowires as green light emitting at nanowire tips. When the nanowire is excited in a position (red circles in **Figure 1d**), the nanowire is served as microcavity where PL signals oscillate in the micro-cavity and finally leak out at the two ends of the nanowire. Guided PL signal collected at one end of nanowire (green circles in **Figure 1d**) is shown in **Figure 1e.** The asymmetrical PL line shape and red shift of emission peak compared to in-situ excited PL spectra have been attributed to re-absorption of high energy photons and F-P mode guiding of low energy photons, [45-46] which can be evidenced from the propagation loss spectrum in **Note2**. The mode spacing of the interference peaks is inversely proportional to nanowire length (see *Supporting Information,* **Note3**), demonstrating that the nanowire functions as an optical Fabry−Pérot (F-P) resonator along its length. One unique feature of F-P modes in

conventional photonic model is the identical mode spacing toward different energy region due to the group index almost keep a constant for different energy. While the value of mode spacing decreases from 2.83 nm (11 meV) to 1.56 nm (5 meV) as the mode energy increases from 565 nm (2.21 eV) to 533 nm (2.33 eV). This oscillation mode cannot be explained by conventional photonic model, suggesting strong light–matter interaction happened in $CsPbBr_3$ nanowires and the formation of exciton-polaritons quasi-particles.[17, 47-49] Thus, the observed series of resonance peaks on the PL spectrum could be attributed to the polariton emission. Actually, the stability of exciton-polariton is determined by the exciton binding energy.[50-51] The exciton binding energy of $CsPbBr_3$ is 38~60 meV[16, 38] (see *Supporting Information*, **Figure S8**), which is higher than the thermal disturbance at room temperature ($k_BT$~ 26 meV). Hence, robust exciton of $CsPbBr_3$ facilitates the formation of exciton-polaritons that can travel back and forth along the nanowire axis coherently, making this PL guiding and microcavity oscillation more efficiently at room temperature.

The cavity modulated spectroscopy of $CsPbBr_3$ nanowires shown in **Figure 1e** can be fitted by a series of Lorentzian line shapes (short dot lines). Energy-wavevector dispersion curves in the z-direction (along nanowire length) of $CsPbBr_3$ nanowires are shown in **Figure 1f**. The shape of the mode dispersion can be determined from the maxima of F-P resonant polariton modes which are equally spaced at integral multiples of $\pi/L_z$ in wavevector space, as the scatter data points in **Figure 1f**. It is obvious that the mode dispersion curves determined by the

experimental results show significant curvature deviating from the purely photonic model.[17] The solid lines represent numerical solutions for the eigenvalue equation of a dielectric triangular prism waveguide using a phenomenological equation for $CsPbBr_3$ permittivity (*Supporting Information*, **Note5**). In wavevector space, the upper polariton branch (UPB) is severely damped and these modes are actually situated on lower polariton branch (LPB) of exciton-polariton dispersion curves. The UPB severely damped at these energies can be explained as the dynamic of reservoir excitons created by non-resonant high-energy excitation.[52] The excited UPB population scatter to the exciton reservoir, results in a fast non-radiative depopulation of the UPB.[53] The reserved excitons further scatter into LPB states through phonon emission. Energy-wavevector dispersion can be well fitted by coupled oscillator model of polaritons. The coupling strength of exciton to the fundamental guided optical mode is displayed by the smallest energy difference between upper and lower polariton branch, *i.e.*, Rabi splitting energy as indicated by the red arrow in **Figure 1f**. Numerical calculations and a histogram for almost one hundred nanowires of coupling strength are given in *Supporting Information*, **Note6.**

The cavity modulated spectroscopy of different size of $CsPbBr_3$ nanowires (with widths of 3.31, 1.99, 1.19 and 0.78 μm and lengths of 11.01, 14.02, 16.41 and 20.77 μm respectively) shown in **Figure 2a-d.** This length-dependent phenomenon can be seen more clearly in the **Note3** of *Supporting Information*. Aside from the different interference peak spacing caused by the different nanowire lengths, the whole polariton emission spectra shows red shift of 7 meV and 18 meV for 16.9 μm and

24.1 μm length of nanowires compared to nanowire of 10.1 μm, indicating enhanced polariton relaxation before polariton emission from edge of $CsPbBr_3$ crystal. Fitting result of Rabi splitting energy for nanowires in **Figure 2a-d** dramatically increased from 401 to 656 meV shown in **Figure 2e-h**. Rabi splitting energy of 656 meV is obviously much larger than that in most inorganic semiconductor materials [54] (~200 meV for CdS; ~150 meV for ZnO) and $CsPbCl_3$ nanoplatelets in DBR microcavity (265 meV),[18] indicating large oscillator strength. A comparison of $CsPbBr_3$ and traditional semiconductors (ZnO and CdS) in oscillator strength is summarized in **Table 1**. This can be advantaged for stable polariton state up to or beyond room temperature so long as vacuum Rabi frequency ($\Omega/\hbar$) is larger than the exciton dephasing rate.[54] We should note that even the length of nanowires in Figure **2b-d** increase to 14.02, 16.41 and 20.77 μm, the geometric volume decrease from 24.96 to 2.59 $\mu m^3$, suggesting that the micro/nanowire dimension plays an important role in altering light-matter coupling strength. To illuminate the role of individual nanowire dimension playing on the exciton-polariton coupling strength, the electric-field properties of F-P microcavity with different nanowire dimensions are investigated with the finite difference eigenmode solver in Mode Solution (S*upporting Information*, **Note7**). The normalized electric-field distribution $|E|^2$ at 540 nm of $CsPbBr_3$ nanowires with different cross-section area are described in the insets of **Figure 2e-h**. The electric-field distribution at the cross-section for the four given nanowires reveals that the energy of electric field is well confined in the nanowires, and the scattering into the surrounding air and substrate is quite limited. Lateral confinement of

nanowire lead to the decrease of effective volume in smaller cross-section nanowires. However, when the cross-section reduces further (0.04 μm$^2$ in our experiment), the electric field begin to scatter into the air and the substrate to some extent resulting in the decrease of light-matter coupling strength (*Supporting Information,* **Figure S10**).

The group refractive index $n_g$ along the nanowire is calculated by $v_{g=}\frac{d\omega}{dk_{\|}}$ and $n_{g=}\frac{c}{v_g}$.[55] Plots of wavelength dependence of group refractive index $n_g$ for nanowires with Rabi splitting energy of 401 meV, 440 meV, 499 meV and 656 meV are shown in **Figure 3a**, which indicates that $n_g$ is about 3 at longer wavelength for four nanowires and suddenly increases up to 15 for nanowire with Rabi splitting energy of 401 meV and 21 for nanowire with Rabi splitting energy of 656 meV at shorter wavelength. The enhancement group refractive index shows strong dispersion in high photon energy bands, which is characteristic of exciton-polariton from the strong coupling between excitons and photons (A detailed analysis in *Supporting Information,* **Note8**).[19, 48, 56] Then, we summarized the results for the Rabi frequency, *g* and Rabi splitting energy, *versus* effective mode volume for nanowire waveguides with diameters ranging from 160–3500 nm and lengths ranging from 2.45 to 21 μm in **Figure 3b** (calculation methods are available in *Supporting Information,* **Note7**). Herein we use the effective mode volume instead of the mode volume to quantify the average field strength instead of the maximum field strength since excitons occur throughout the whole nanowire.[30] When the effective volume is larger than 10 μm$^2$, the Rabi frequency *g* and the Rabi splitting energy present lower value, and increase slowly with the $V_{eff}$ decrease from 100 to 10 μm$^{-3}$. However, with the further decrease

of the $V_{eff}$, the Rabi frequency $g$ increases sharply by up to 2.4 times where coupling strength is strongly enhanced in this cavity. This strongly proved the size-dependent coupling strength. The relation between Rabi splitting energy and effective volume in this small effective volume region can be fitted by equation **S1** with effective oscillator strength $n(V) \times f(V)$ of $1.4915 \times 10^{10}$ as a fit parameter (the red dash dot curve line in **Figure 3b**), indicating that oscillator strength is significantly increased with the decreasing number of oscillators.

We analyzed the essential reason of the remarkable enhancement of light-matter coupling strength in the $CsPbBr_3$ nanowire microcavities. Firstly, the decrease of the effective mode volume could increase the electromagnetic energy density in the nanowire cavity, directly resulting in coupling strength increased. Secondly, considering the high ordering of $CsPbBr_3$ due to the distinct size and charge of the Cs and Pb ions,[13] the coherently filling of exciton wavefunction in nanocrystals is promoted until scattering limits the exciton coherence volume.[57] This enhancement of exciton oscillator strength presented in the inset of **Figure 3b** has also been observed in CdSe,[58] ZnO quantum dots[59] and CdS nanowire[30] when the crystal dimension approaches the wavelength of light. In this regard, several oscillators coherently combine into one larger dipole mediated by coupling to the same optical mode. In addition, we also carried out the temperature-dependent studies and associated fitting. (*Supporting Information,* **Note9**) Our conclusion of Rabi splitting energy changing with temperature is inconsistent with that reported before,[36] which is needed further study.

Polariton lasers act as coherent light sources very similar to conventional lasers, the main difference being that polariton lasing occurs without necessary for population inversion, deriving from the formation mechanism of stimulated relaxation of polaritons [60] as opposed to stimulated emission of photons. As a consequence, it has been predicted and observed that the threshold for polariton lasing is several orders of magnitude smaller than the conventional photon lasing threshold.[61-63] Given this, we delved deeper into the lasing behaviors, the influence of exciton-polariton coupling strength on the lasing behaviors and mechanism. **Figure 4a** depicts the PL spectra of a $CsPbBr_3$ nanowire with L=12.4 μm, as a function of pump fluences. The PL emission shows a clearly nonlinear behavior: at low pump fluence of 3 μJ/cm$^2$, the PL spectrum displays broad spontaneous emission at 525 nm. Upon increasing the pump fluence from 6 μJ/cm$^2$ to 8 μJ/cm$^2$, strong laser emission develops as a set of sharp peaks at the right shoulder of spontaneous emission peak, indicating the polariton resonant cavity modes. With further increase of pump fluence, these modes become dominant in the PL spectra, as indicated by the orange line in **Figure 4a** recorded at 10 μJ/cm$^2$. And the individual cavity mode presents a line-width as narrow as 0.4 nm. **Figure 4b** shows the bright-field optical microscopy image (down) and emission images at low (middle) and high (top) pump fluence of a typical $CsPbBr_3$ nanowire. Compared with the uniform emission from the entire nanowire under low pump fluence, a strong emission was observed at both ends with the high pump fluence, indicating the transition from random spontaneous emission to directional stimulated radiation. At the same time, we can distinguish the interference

pattern from the two ends in this emission image, which is the evident of coherent light. Each pattern is thought to be resulted from the interference of diffracted coherent light escaping from two ends of the nanowire cavity.[11, 15, 64] **Figure 4c** shows the emission intensities as a function of pump fluence in a log-log scale, showing clearly an intersection point at $P_{th}$ = 8 μJ/cm$^2$ defined as the lasing threshold. A typical "*S*" shape power dependent emission relationship also indicates a transition from a sublinear regime to a superlinear regime.[8, 65] Meanwhile, a slight broadening of the FWHM below threshold is also observed as the recently work by Su *et.al.*,[18] which is attributed to exciton - polariton interaction. Then, the FWHM dramatically decreases from 20 nm at 6 μJ/cm$^2$ to 0.4 nm at 10 μJ/cm$^2$, indicating a sharp increase of the temporal coherence.

**Figure 5a-c** depicts the comparison of the lasing spectra and the guided PL spectra for three different coupling strengths with Rabi splitting of 357 meV, 434 meV, 554 meV. It is found that the lasing modes of the three $CsPbBr_3$ nanowires observed above threshold are in different positions comparing with those guided F-P modes observed below threshold. Specifically, the lasing spectrum sited at the left of the peak of its corresponding waveguide mode spectrum for nanowire with Rabi splitting of 357meV in **Figure 5a**; the lasing spectrum located at the middle of the peak of the corresponding waveguide mode spectrum for nanowire with Rabi splitting of 434meV in **Figure 5b**; the position of the lasing spectrum is a little right relative to the peak of its corresponding waveguide mode spectrum for nanowire with Rabi splitting of 554meV in **Figure 5c**. The overlap range between multiple F-P

interference peaks and lasing peaks is larger with the coupling strength increasing, meaning the increasing proportion of polariton in the lasing spectra. By further analyzing, the lasing modes were found to be occurred in lower energy for larger coupling strength comparing with corresponding guided PL spectrum. It means that the more efficient cooling of the polaritons by acoustic phonon scattering moves the condensate state further down the bottleneck region on the LPB.[54, 66] The increased relaxation efficiency has been attributed to the larger excitonic character of the exciton-polaritons in the LPB as discussed by Coles *et al.*[67] A larger excitonic fraction improves relaxation due to increased polariton lifetime and the resulting flatter dispersion supports polatiton-phonon scattering. [68] Also, the overall relative redshift of lasing modes with Rabi splitting increase is consistent with the redshift of maximum polariton emission by increasing the Rabi splitting. [69] We summarize the threshold evolution versus the Rabi splitting in **Figure 5d**. The threshold appears to be minishing greatly when the Rabi splitting increased as the eye-guided line indicates. The threshold of the nanowire laser with Rabi splitting of ~550 meV is one order of magnitude smaller than that of nanowire with Rabi splitting of ~350 meV. The dramatical reduction of the laser thresholds is an unambiguous (although indirect) evidence that the lasing is from the polariton resonances for the nanowire with strong coupling, and we are indeed in presence of both polariton lasing (with Rabi splitting larger than ~ 500 meV), and conventional photon lasing (with Rabi splitting smaller ~ 400 meV). Moreover, the discovery of lasing mode blueshift with the increase of pump fluence and different quantity of blueshift for nanowires with different Rabi

splitting give us the further evidence of polariton lasing. (*Supporting Information,* **Note10**)

## CONCLUSION

In summary, $CsPbBr_3$ perovskite micro/nanowires were synthesized by chemical vapor deposition method. Using scanning-excitation single nanowire emission spectroscopy with a laser as a spatially resolved excitation source, we observe standing-wave exciton-polariton in the $CsPbBr_3$ nanowires. The Rabi splitting and group index can be tunable by the varied dimensions of the nanowires. Thus, the observation of polariton lasing with exceptionally large vacuum Rabi splitting of 656 meV and almost one order of magnitude low threshold opens the door not only to low power coherent light sources and model systems for polaritonics, but also to a better understanding of this class of material in optoelectronics applications.

## Methods

***Characterization of $CsPbBr_3$ nanowires***: The morphology of the as-grown samples were characterized using AFM (Veeco Dimension 3100) in the tapping mode, scanning electron microscopy (SEM, NOVA NanoSEM 430) equipped with Energy Disperse Spectroscopy (EDS, Oxford: X-Max80), X-ray powder diffraction (XRD, D/max-TTRIII, Cu $K\alpha$ radiation) in the $\theta-2\theta$ geometry, and an optical microscope (Olympus BX53),. Absorption spectra were measured by the optical microscope equipped with a halogen lamp, operating in transmission mode.

***Steady-State and spatial resolved Photoluminescence measurements*:** The steady-state PL spectra measurements were performed with excitation light from a CW laser ( $\lambda$ = 405 nm) and the pumping power was adjusted using neutral density filters. The laser was focused on the sample by a 100× objective lens (NA = 0.95). Backscattered signal was either projected onto a small CCD for color imaging or collected through the focusing lens into an optical fiber that was coupled to a Princeton Instrument SP2500i spectrometer with a liquid nitrogen cooled charge coupled device detector. A pin hole fixed on two dimensional stages was arranged before backscattered signal could be projected to CCD or optical fiber. Light could be collected from specific parts of the nanowire with a spatial resolution of ~200 nm.

***Lasing Spectroscopy**:* The lasing spectroscopy was carried out on the optical microscope (Olympus BX53). A 400 nm pulsed laser was used as the excitation source, which was frequency doubled by a BBO crystal from an amplifier laser source. The amplifier laser source was the 800 nm laser pulses which were from a Coherent Astrella regenerative amplifier (80 fs, 1 kHz, 2.5 mJ/pulse), seeded by a Coherent Vitara-s oscillator (35 fs, 80 MHz). The 400 nm wavelength laser pulses were focused on the sample with a 10× objective lens (NA = 0.35). All the other optical paths are identical to steady-state PL measurements.

## ASSOCIATED CONTENT

*Supporting Information*. Chemical vapor deposition and characterization, spatially resolved PL and propagation loss spectrum, confirmation of Fabry-Pérot cavity mode, fitting of exciton binding energy, the exciton-polariton model and fitting of the dispersion curve, mode simulation and effective volume, numerical calculations of coupling strength of $CsPbBr_3$ nanowires, group index of a $CsPbBr_3$ nanowire modeled with different coupling strength, temperature-dependent study of Rabi splitting energy, power dependent lasing energy blueshift, and oscillator strengths of different semiconductor materials. This material is available free of charge via the Internet at http://pubs.acs.org.

**Competing financial interests**

The authors declare no competing financial interests.

**ACKNOWLEDGMENTS**

X.F.L thanks the support from the Ministry of Science and Technology (No.2016YFA0200700 and 2017YFA0205004), National Natural Science Foundation of China (No.21673054), Open Project of Key Laboratory for UV-emitting Materials and Technology of Ministry of Education (130028699) and Beijing Natural Science Foundation (4182076). Q.Z. acknowledges the support of start-up funding from Peking University, one-thousand talent programs from Chinese government, open research fund program of the state key laboratory of low-dimensional quantum physics. Q.Z. also thanks funding support from the Ministry of Science and Technology (2017YFA0205700; 2017YFA0304600). This work is also supported by the National Natural Science Foundation of China (grant numbers 61307120, 61704038, 11474187). We also thank helpful discussion from Prof. Xiong from Nanyang Technological University.

**References:**

(1) Gratzel, M., The light and shade of perovskite solar cells. *Nat. Mater.* **2014,** *13*, 838-42.
(2) Mei, A.; Li, X.; Liu, L.; Ku, Z.; Liu, T.; Rong, Y.; Xu, M.; Hu, M.; Chen, J.; Yang, Y.; Gratzel, M.; Han, H., A hole-conductor-free, fully printable mesoscopic perovskite solar cell with high stability. *Science* **2014,** *345*, 295-8.
(3) Park, N. G., Organometal Perovskite Light Absorbers Toward a 20% Efficiency Low-Cost Solid-State Mesoscopic Solar Cell. *J. Phys. Chem. Lett.* **2013,** *4*, 2423-2429.
(4) Snaith, H. J., Perovskites: The Emergence of a New Era for Low-Cost, High-Efficiency Solar Cells. *J. Phys. Chem. Lett.* **2013,** *4*, 3623-3630.
(5) Zhou, H.; Chen, Q.; Li, G.; Luo, S.; Song, T. B.; Duan, H. S.; Hong, Z.; You, J.; Liu, Y.; Yang, Y., Photovoltaics. Interface engineering of highly efficient perovskite solar cells. *Science* **2014,** *345*, 542-6.
(6) Yang, W. S.; Park, B.-W.; Jung, E. H.; Jeon, N. J.; Kim, Y. C.; Lee, D. U.; Shin, S. S.; Seo, J.; Kim, E. K.; Noh, J. H.; Seok, S. I., Iodide management in formamidinium-lead-halide–based perovskite layers for efficient solar cells. *Science* **2017,** *356*, 1376-1379.
(7) Li, X. M.; Cao, F.; Yu, D. J.; Chen, J.; Sun, Z. G.; Shen, Y. L.; Zhu, Y.; Wang, L.; Wei, Y.; Wu, Y.; Zeng, H. B., All Inorganic Halide Perovskites Nanosystem: Synthesis, Structural Features, Optical Properties and Optoelectronic Applications. *Small* **2017,** *13*, 1603996.
(8) Liu, X.; Ha, S. T.; Zhang, Q.; de la Mata, M.; Magen, C.; Arbiol, J.; Sum, T. C.; Xiong, Q., Whispering Gallery Mode Lasing from Hexagonal Shaped Layered Lead Iodide Crystals. *ACS Nano* **2015,** *9*, 687-695.
(9) Wang, Y.; Li, X. M.; Song, J. Z.; Xiao, L.; Zeng, H. B.; Sun, H. D., All-Inorganic Colloidal Perovskite Quantum Dots: A New Class of Lasing Materials with Favorable Characteristics. *Adv. Mater.* **2015,** *27*, 7101-7108.
(10) Zhang, Q.; Su, R.; Du, W.; Liu, X.; Zhao, L.; Ha, S. T.; Xiong, Q., Advances in Small Perovskite-Based Lasers. *Small Methods* **2017,** *1*, 1700163.
(11) Zhu, H.; Fu, Y.; Meng, F.; Wu, X.; Gong, Z.; Ding, Q.; Gustafsson, M. V.; Trinh, M. T.; Jin, S.; Zhu, X. Y., Lead halide perovskite nanowire lasers with low lasing thresholds and high quality factors. *Nat. Mater.* **2015,** *14*, 636-42.
(12) Kulbak, M.; Cahen, D.; Hodes, G., How Important Is the Organic Part of Lead Halide Perovskite Photovoltaic Cells? Efficient CsPbBr3 Cells. *J. Phys. Chem. Lett.* **2015,** *6*, 2452-2456.
(13) Protesescu, L.; Yakunin, S.; Bodnarchuk, M. I.; Krieg, F.; Caputo, R.; Hendon, C. H.; Yang, R. X.; Walsh, A.; Kovalenko, M. V., Nanocrystals of Cesium Lead Halide Perovskites (CsPbX(3), X = Cl, Br, and I): Novel Optoelectronic Materials Showing Bright Emission with Wide Color Gamut. *Nano Lett.* **2015,** *15*, 3692-6.
(14) Yakunin, S.; Protesescu, L.; Krieg, F.; Bodnarchuk, M. I.; Nedelcu, G.; Humer, M.; De Luca, G.; Fiebig, M.; Heiss, W.; Kovalenko, M. V., Erratum: Low-threshold amplified spontaneous emission and lasing from colloidal nanocrystals of caesium lead halide perovskites. *Nat. Commun.* **2015,** *6*, 8515.

(15) Eaton, S. W.; Lai, M. L.; Gibson, N. A.; Wong, A. B.; Dou, L. T.; Ma, J.; Wang, L. W.; Leone, S. R.; Yang, P. D., Lasing in robust cesium lead halide perovskite nanowires. *Proc. Natl. Acad. Sci. USA* **2016,** *113*, 1993-1998.
(16) Zhang, Q.; Su, R.; Liu, X.; Xing, J.; Sum, T. C.; Xiong, Q., High-Quality Whispering-Gallery-Mode Lasing from Cesium Lead Halide Perovskite Nanoplatelets. *Adv. Funct. Mater.* **2016,** *26*, 6238-6245.
(17) Park, K.; Lee, J. W.; Kim, J. D.; Han, N. S.; Jang, D. M.; Jeong, S.; Park, J.; Song, J. K., Light-Matter Interactions in Cesium Lead Halide Perovskite Nanowire Lasers. *J. Phys. Chem. Lett.* **2016,** *7*, 3703-3710.
(18) Su, R.; Diederichs, C.; Wang, J.; Liew, T. C. H.; Zhao, J.; Liu, S.; Xu, W.; Chen, Z.; Xiong, Q., Room-Temperature Polariton Lasing in All-Inorganic Perovskite Nanoplatelets. *Nano Lett.* **2017,** *17*, 3982-3988.
(19) Hopfield, J. J., Theory of the Contribution of Excitons to the Complex Dielectic Constant of Crystals. *Phys. Rev.* **1958,** *112*, 1555-1567.
(20) Thomas, D. G.; Hopfield, J. J., Exciton Spectrum of Cadmium Sulfide. *Phys. Rev.* **1959,** *116*, 573-582.
(21) Fraser, M. D.; Hofling, S.; Yamamoto, Y., Physics and applications of exciton-polariton lasers. *Nat. Mater.* **2016,** *15*, 1049-52.
(22) Lagoudakis, K. G.; Wouters, M.; Richard, M.; Baas, A.; Carusotto, I.; Andre, R.; Dang, L. E. S. I.; Deveaud-Pledran, B., Quantized vortices in an exciton-polariton condensate. *Nat. Phys.* **2008,** *4*, 706-710.
(23) Amo, A.; Sanvitto, D.; Laussy, F. P.; Ballarini, D.; del Valle, E.; Martin, M. D.; Lemaitre, A.; Bloch, J.; Krizhanovskii, D. N.; Skolnick, M. S.; Tejedor, C.; Vina, L., Collective fluid dynamics of a polariton condensate in a semiconductor microcavity. *Nature* **2009,** *457*, 291-295.
(24) Nitsche, W. H.; Kim, N. Y.; Roumpos, G.; Schneider, C.; Kamp, M.; Hofling, S.; Forchel, A.; Yamamoto, Y., Algebraic order and the Berezinskii-Kosterlitz-Thouless transition in an exciton-polariton gas. *Phys. Rev. B* **2014,** *90*, 205430.
(25) Balili, R.; Hartwell, V.; Snoke, D.; Pfeiffer, L.; West, K., Bose-einstein condensation of microcavity polaritons in a trap. *Science* **2007,** *316*, 1007-1010.
(26) Stevenson, R. M.; Astratov, V. N.; Skolnick, M. S.; Whittaker, D. M.; Emam-Ismail, M.; Tartakovskii, A. I.; Savvidis, P. G.; Baumberg, J. J.; Roberts, J. S., Continuous wave observation of massive polariton redistribution by stimulated scattering in semiconductor microcavities. *Phys. Rev. Lett.* **2000,** *85*, 3680-3683.
(27) Graf, A.; Held, M.; Zakharko, Y.; Tropf, L.; Gather, M. C.; Zaumseil, J., Electrical pumping and tuning of exciton-polaritons in carbon nanotube microcavities. *Nat. Mater.* **2017,** *16*, 911-917.
(28) Reithmaier, J. P.; Sek, G.; Loffler, A.; Hofmann, C.; Kuhn, S.; Reitzenstein, S.; Keldysh, L. V.; Kulakovskii, V. D.; Reinecke, T. L.; Forchel, A., Strong coupling in a single quantum dot-semiconductor microcavity system. *Nature* **2004,** *432*, 197-200.
(29) Andreani, L. C.; Panzarini, G.; Gerard, J. M., Strong-coupling regime for quantum boxes in pillar microcavities: Theory. *Phys. Rev. B* **1999,** *60*, 13276-13279.
(30) van Vugt, L. K.; Piccione, B.; Cho, C.-H.; Nukala, P.; Agarwal, R., One-dimensional polaritons with size-tunable and enhanced coupling strengths in

semiconductor nanowires. *Proc. Natl. Acad. Sci. USA* **2011,** *108*, 10050-10055.
(31) Vahala, K. J., Optical microcavities. *Nature* **2003,** *424*, 839-46.
(32) van Vugt, L. K.; Ruhle, S.; Ravindran, P.; Gerritsen, H. C.; Kuipers, L.; Vanmaekelbergh, D., Exciton polaritons confined in a ZnO nanowire cavity. *Phys. Rev. Lett.* **2006,** *97*, 147401.
(33) van Vugt, L. K.; Piccione, B.; Agarwal, R., Incorporating polaritonic effects in semiconductor nanowire waveguide dispersion. *Appl. Phys. Lett.* **2010,** *97*, 061115.
(34) Zhou, H.; Yuan, S.; Wang, X.; Xu, T.; Wang, X.; Li, H.; Zheng, W.; Fan, P.; Li, Y.; Sun, L.; Pan, A., Vapor Growth and Tunable Lasing of Band Gap Engineered Cesium Lead Halide Perovskite Micro/Nanorods with Triangular Cross Section. *ACS Nano* **2017,** *11*, 1189-1195.
(35) Zhang, S.; Shang, Q.; Du, W.; Shi, J.; Wu, Z.; Mi, Y.; Chen, J.; Liu, F.; Li, Y.; Liu, M.; Zhang, Q.; Liu, X., Strong Exciton-Photon Coupling in Hybrid Inorganic-Organic Perovskite Micro/Nanowires. *Adv. Opt. Mater.* **2018,** *6*, 1701032.
(36) Evans, T. J. S.; Schlaus, A.; Fu, Y.; Zhong, X.; Atallah, T. L.; Spencer, M. S.; Brus, L. E.; Jin, S.; Zhu, X. Y., Continuous-Wave Lasing in Cesium Lead Bromide Perovskite Nanowires. *Adv. Opt. Mater.* **2018,** *6*, 1700982.
(37) Menard, J. M.; Poellmann, C.; Porer, M.; Leierseder, U.; Galopin, E.; Lemaitre, A.; Amo, A.; Bloch, J.; Huber, R., Revealing the dark side of a bright exciton-polariton condensate. *Nat. Commun.* **2014,** *5*, 4648.
(38) Sestu, N.; Cadelano, M.; Sarritzu, V.; Chen, F.; Marongiu, D.; Piras, R.; Mainas, M.; Quochi, F.; Saba, M.; Mura, A.; Bongiovanni, G., Absorption F-sum rule for the exciton binding energy in methylammonium lead halide perovskites. *J. Phys. Chem. Lett.* **2015,** *6*, 4566-72.
(39) Li, J.; Luo, L.; Huang, H.; Ma, C.; Ye, Z.; Zeng, J.; He, H., 2D Behaviors of Excitons in Cesium Lead Halide Perovskite Nanoplatelets. *J. Phys. Chem. Lett.* **2017,** *8*, 1161-1168.
(40) Wang, Y.; Sun, X.; Shivanna, R.; Yang, Y.; Chen, Z.; Guo, Y.; Wang, G. C.; Wertz, E.; Deschler, F.; Cai, Z.; Zhou, H.; Lu, T. M.; Shi, J., Photon Transport in One-Dimensional Incommensurately Epitaxial CsPbX3 Arrays. *Nano Lett.* **2016,** *16*, 7974-7981.
(41) Fu, Y.; Zhu, H.; Stoumpos, C. C.; Ding, Q.; Wang, J.; Kanatzidis, M. G.; Zhu, X.; Jin, S., Broad Wavelength Tunable Robust Lasing from Single-Crystal Nanowires of Cesium Lead Halide Perovskites (CsPbX3, X = Cl, Br, I). *ACS Nano* **2016,** *10*, 7963-7972.
(42) Ravi, V. K.; Markad, G. B.; Nag, A., Band Edge Energies and Excitonic Transition Probabilities of Colloidal CsPbX3 (X = Cl, Br, I) Perovskite Nanocrystals. *ACS Energy Lett.* **2016,** *1*, 665-671.
(43) Zhang, D. D.; Yang, Y. M.; Bekenstein, Y.; Yu, Y.; Gibson, N. A.; Wong, A. B.; Eaton, S. W.; Kornienko, N.; Kong, Q.; Lai, M. L.; Alivisatos, A. P.; Leone, S. R.; Yang, P. D., Synthesis of Composition Tunable and Highly Luminescent Cesium Lead Halide Nanowires through Anion-Exchange Reactions. *J. Am. Chem. Soc.* **2016,** *138*, 7236-7239.
(44) Akkerman, Q. A.; Motti, S. G.; Kandada, A. R. S.; Mosconi, E.; D'Innocenzo, V.;

Bertoni, G.; Marras, S.; Kamino, B. A.; Miranda, L.; De Angelis, F.; Petrozza, A.; Prato, M.; Manna, L., Solution Synthesis Approach to Colloidal Cesium Lead Halide Perovskite Nanoplatelets with Monolayer-Level Thickness Control. *J. Am. Chem. Soc.* **2016,** *138*, 1010-1016.
(45) Zhang, C.; Zou, C. L.; Yan, Y.; Hao, R.; Sun, F. W.; Han, Z. F.; Zhao, Y. S.; Yao, J., Two-photon pumped lasing in single-crystal organic nanowire exciton polariton resonators. *J. Am. Chem. Soc.* **2011,** *133*, 7276-9.
(46) Piccione, B.; van Vugt, L. K.; Agarwal, R., Propagation loss spectroscopy on single nanowire active waveguides. *Nano Lett.* **2010,** *10*, 2251-6.
(47) Wang, X.; Liao, Q.; Xu, Z.; Wu, Y.; Wei, L.; Lu, X.; Fu, H., Exciton-Polaritons with Size-Tunable Coupling Strengths in Self-Assembled Organic Microresonators. *ACS Photonics* **2014,** *1*, 413-420.
(48) van Vugt, L. K.; Zhang, B.; Piccione, B.; Spector, A. A.; Agarwal, R., Size-dependent waveguide dispersion in nanowire optical cavities: slowed light and dispersionless guiding. *Nano Lett.* **2009,** *9*, 1684-8.
(49) Liao, Q.; Xu, Z.; Zhong, X.; Dang, W.; Shi, Q.; Zhang, C.; Weng, Y.; Li, Z.; Fu, H., An organic nanowire waveguide exciton–polariton sub-microlaser and its photonic application. *J. Mater. Chem. C* **2014,** *2*, 2773-2778.
(50) Takazawa, K.; Inoue, J.; Mitsuishi, K.; Takamasu, T., Fraction of a millimeter propagation of exciton polaritons in photoexcited nanofibers of organic dye. *Phys. Rev. Lett.* **2010,** *105*, 067401.
(51) Scholes, G. D.; Rumbles, G., Excitons in nanoscale systems. *Nat. Mater.* **2006,** *5*, 683-96.
(52) Lidzey, D. G.; Fox, A. M.; Rahn, M. D.; Skolnick, M. S.; Agranovich, V. M.; Walker, S., Experimental study of light emission from strongly coupled organic semiconductor microcavities following nonresonant laser excitation. *Phys. Rev. B* **2002,** *65*, 195312.
(53) Virgili, T.; Coles, D.; Adawi, A. M.; Clark, C.; Michetti, P.; Rajendran, S. K.; Brida, D.; Polli, D.; Cerullo, G.; Lidzey, D. G., Ultrafast polariton relaxation dynamics in an organic semiconductor microcavity. *Phys. Rev. B* **2011,** *83*.
(54) Sanvitto, D.; Kena-Cohen, S., The road towards polaritonic devices. *Nat. Mater.* **2016,** *15*, 1061-73.
(55) Sun, L.; Chen, Z.; Ren, Q.; Yu, K.; Bai, L.; Zhou, W.; Xiong, H.; Zhu, Z. Q.; Shen, X., Direct observation of whispering gallery mode polaritons and their dispersion in a ZnO tapered microcavity. *Phys. Rev. Lett.* **2008,** *100*, 156403.
(56) Thevenaz, L., Slow and fast light in optical fibres. *Nat. Photonics* **2008,** *2*, 474-481.
(57) van Vugt, L. K., Optical properties of semiconducting nanowires. *PhD thesis* **2007**.
(58) Scheibner, M.; Schmidt, T.; Worschech, L.; Forchel, A.; Bacher, G.; Passow, T.; Hommel, D., Superradiance of quantum dots. *Nat. Phys.* **2007,** *3*, 106-110.
(59) Gil, B.; Kavokin, A. V., Giant exciton-light coupling in ZnO quantum dots. *Appl. Phys. Lett.* **2002,** *81*, 748-750.
(60) Malpuech, G.; Kavokin, A.; Di Carlo, A.; Baumberg, J. J., Polariton lasing by

exciton-electron scattering in semiconductor microcavities. *Phys. Rev. B* **2002,** *65*, 153310.
(61) Kasprzak, J.; Richard, M.; Kundermann, S.; Baas, A.; Jeambrun, P.; Keeling, J. M.; Marchetti, F. M.; Szymańska, M. H.; André, R.; Staehli, J. L., Bose-Einstein condensation of exciton polaritons. *Nature* **2006,** *443*, 409.
(62) Porras, D.; Ciuti, C.; Baumberg, J. J.; Tejedor, C., Polariton dynamics and Bose-Einstein condensation in semiconductor microcavities. *Phys. Rev. B* **2002,** *66*, 085304.
(63) Azzini, S.; Gerace, D.; Galli, M.; Sagnes, I.; Braive, R.; Lemaitre, A.; Bloch, J.; Bajoni, D., Ultra-low threshold polariton lasing in photonic crystal cavities. *Appl. Phys. Lett.* **2011,** *99*, 111106.
(64) van Vugt, L. K.; Ruhle, S.; Vanmaekelbergh, D., Phase-correlated nondirectional laser emission from the end facets of a ZnO nanowire. *Nano Lett.* **2006,** *6*, 2707-11.
(65) Zhang, Q.; Ha, S. T.; Liu, X.; Sum, T. C.; Xiong, Q., Room-Temperature Near-Infrared High-Q Perovskite Whispering-Gallery Planar Nanolasers. *Nano Lett.* **2014,** *14*, 5995-6001.
(66) Bajoni, D., Polariton lasers. Hybrid light–matter lasers without inversion. *J. Phys. D: Appl. Phys.* **2012,** *45*, 4211-4216.
(67) Coles, D. M.; Grant, R. T.; Lidzey, D. G.; Clark, C.; Lagoudakis, P. G., Imaging the polariton relaxation bottleneck in strongly coupled organic semiconductor microcavities. *Phys. Rev. B* **2013,** *88*, 3925-3938.
(68) Deng, H.; Chen, J. R.; Lin, S. C.; Wang, S. C.; Lu, T. C.; Hsieh, W. F.; Wu, Y. C., Characteristics of exciton-polaritons in ZnO-based hybrid microcavities. *Opt. Express* **2011,** *19*, 4101-12.
(69) Graf, A.; Tropf, L.; Zakharko, Y.; Zaumseil, J.; Gather, M. C., Near-infrared exciton-polaritons in strongly coupled single-walled carbon nanotube microcavities. *Nat. Commun.* **2016,** *7*, 13078.

## Figure and captions

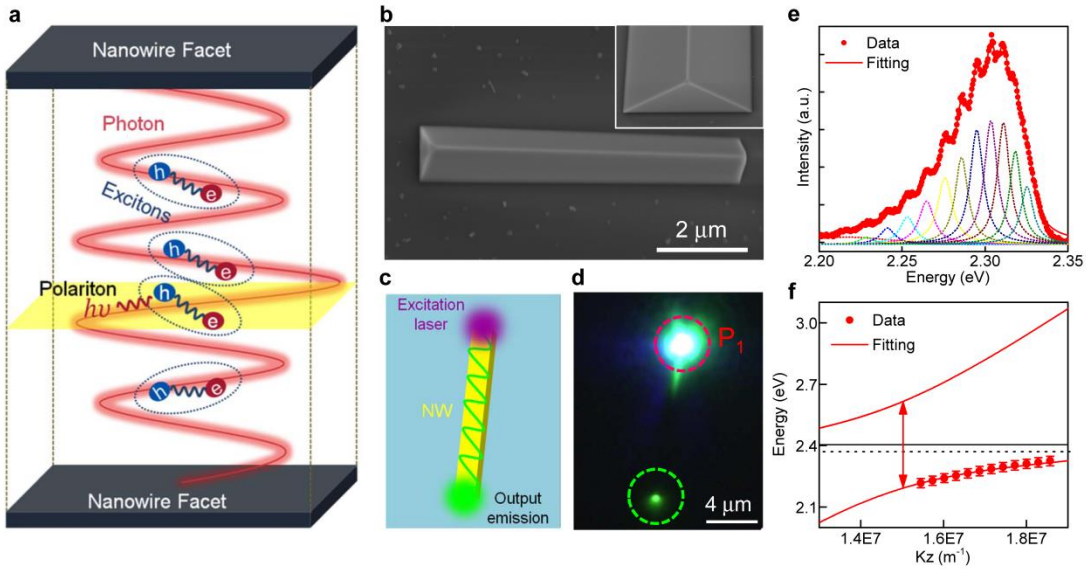


**Figure 1| Schematic of PL probing of cavity exciton-polaritons. (a)** Polaritons emerge from strong coupling between the exciton and the photonic mode of a micro/nanowire cavity. **(b)** SEM image of a representative being investigated tri-prism $CsPbBr_3$ nanowire on the $SiO_2$ substrate. The top right inset is a magnified SEM image showing flat end facets and triangular cross section. **(c)** Diagram of the experimental setup showing a $CsPbBr_3$ nanowire laying on the substrate. The nanowire is excited at the upper end and only the waveguided polaritonic emission is collected at the lower end, in order to resolve the Fabry-Pérot cavity modes. **(d)** Corresponding optical micrograph of the PL resulting from exciting the $CsPbBr_3$ nanowire from the upper point outlined by red dash circle. A clear polaritonic emission spot can be seen at the both end of the $CsPbBr_3$ nanowire which is caused by guiding from the exciting point. **(e)** PL emission spectra of the waveguided emission and **(f)** corresponding energy-wavevector dispersion curves in the z-direction (along nanowire length). The scatter data points indicate the Fabry-Pérot maxima, which have been placed in wavevector space at integer values of $\pi/L_z$. The solid lines are the results of numerical solutions for the eigenvalue equation of a dielectric triangular prism using a phenomenological equation for $CsPbBr_3$ permittivity including light-matter coupling with the $CsPbBr_3$ exciton (dotted horizontal line). Importantly, the Rabi splitting is shown by the arrows indicating $\Delta=2\times\hbar g$.

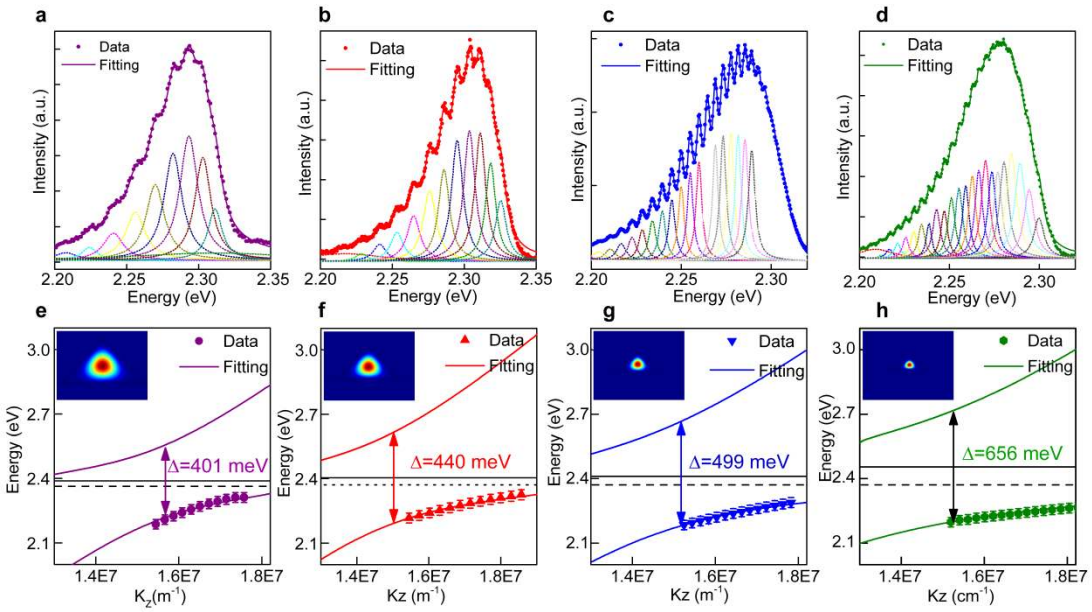


**Figure 2| Size-dependent light-matter coupling strength in $CsPbBr_3$ micro/nanowires (a-d)** Emission spectra acquired from the waveguided end and excited from the other end of $CsPbBr_3$ nanowires with width of 3.31, 1.99, 1.19 and 0.78 μm and lengths of 11.01, 14.02, 16.41 and 20.77 μm, respectively. The spectra show multiple Fabry-Pérot interference peaks which have been fitted by Lorentzian line shapes to determine the resonance energies. **(e–h)** Corresponding energy-wavevector dispersion curves in the *z*-direction (along nanowire length) of above four $CsPbBr_3$ nanowires, respectively. The insets are normalized electric field distribution $|E|^2$ at the cross-section of these four $CsPbBr_3$ nanowires, respectively. The $V_m$ is decreasing with the cross-section of $CsPbBr_3$ nanowires decreasing within the range of our nanowires.

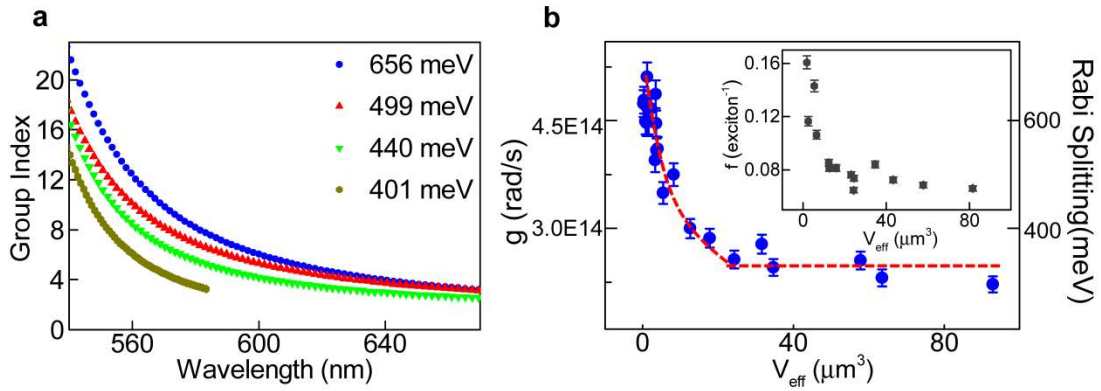


**Figure 3| Numerical mode volume calculations of $CsPbBr_3$ nanowire waveguide cavities. (a)** Wavelength dependence of group refractive index for nanowire with Rabi splitting energy of 401 meV, 440 meV, 499 meV and 656 meV. **(b)** Coupling strength, *g* and Rabi splitting energy, *versus* effective mode volume for 21 nanowire waveguides with diameters ranging from 160–3500 nm and lengths ranging from 2.45 to 21 μm. For larger effective volumes, the coupling strength remains constant. For smaller volumes, the coupling strength *g* increases by up to 2.4 times. Inset is the calculated oscillator strength.

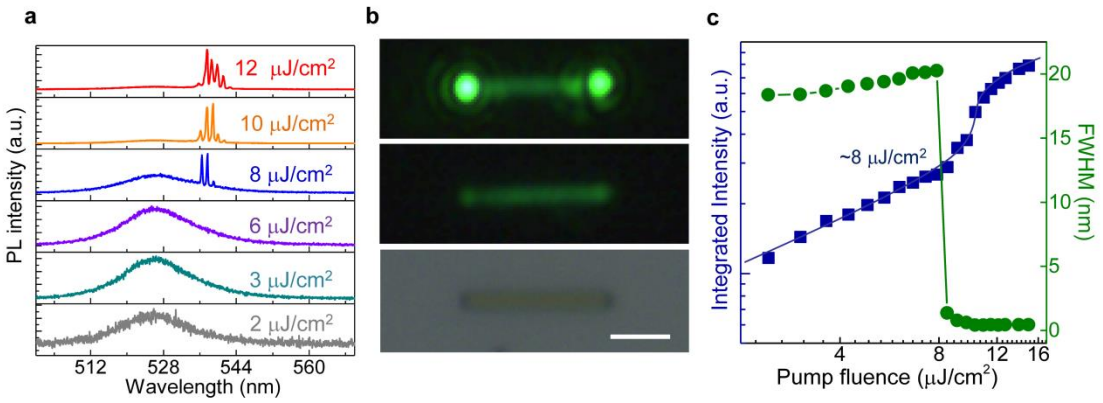


**Figure 4| Characterizations of $CsPbBr_3$ waveguide cavity polariton lasing. (a)** PL spectra of $CsPbBr_3$ nanowire as a function of pump fluence with excitation laser at 400 nm. A sharp increase of emission intensity occurs beyond 1.0 $P_{th}$, suggesting the transition to the nonlinear regime. **(b)** Optical image (down) of a single $CsPbBr_3$ nanowire; the middle and up images show the nanowire emission below and above the threshold $P_{th}$, respectively. **(c)** The power-dependence profile of integrated PL intensities and full width at half maximum (FWHM) as a function of pump fluence. A linewidth narrowing occurs near the threshold of $P_{th}$ = 8 μJ/cm$^2$, along with a sharp increase of emission intensity.

.

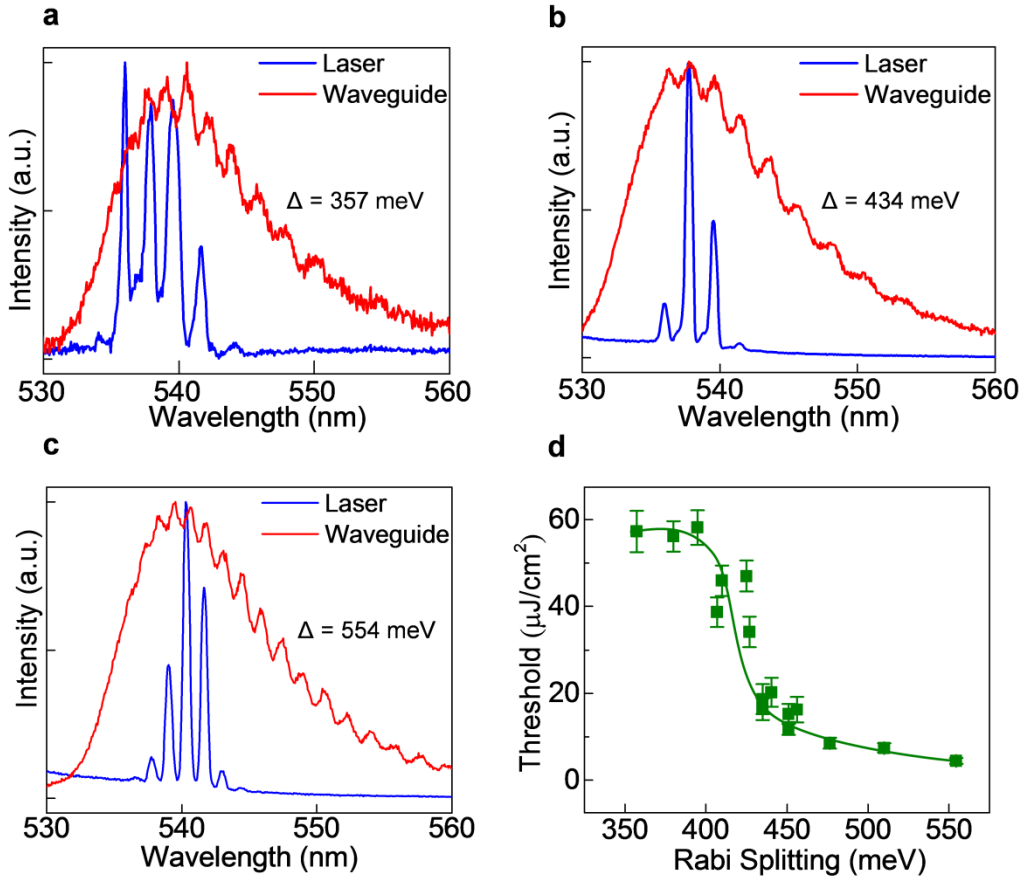


**Figure 5| Lasing behavior of $CsPbBr_3$ nanowires with different Rabi splitting energy. (a-c)** Comparison of lasing spectrum and guided PL spectrum for three different $CsPbBr_3$ nanowires with different coupling strength (Δ represents Rabi splitting) of 357 meV, 434 meV, 554 meV, respectively. The overlap range between multiple Fabry-Pérot interference peaks and lasing peaks located in the splitting region with increasing the coupling strength. **(d)** Measured laser threshold as a function of the Rabi splitting.

**For Table of Contents Use Only**

# Strong Exciton-Photon Coupling and lasing behavior in All-Inorganic $CsPbBr_3$ Micro/nanowire Fabry-Pérot cavity

*Wenna Du,[†,#] Shuai Zhang,[†,‡,#] Jia Shi [†,‡] Jie Chen,[†,‡] Zhiyong Wu,[†] Yang Mi,[†] Zhixiong Liu,[⊥] Yuanzheng Li,[†] Xinyu Sui,[†,‡] Rui Wang,[†] Xiaohui Qiu,[†] Tom Wu,[⊥] Yunfeng Xiao,[ℓ,*] Qing Zhang,[§,*] and Xinfeng Liu[†,‡,*]*

All-inorganic perovskite micro/nanowire hold great promises as nanoscale coherent light source due to their superior optical and electronic properties. The coupling strength between exciton and photon in this system is vital important for their optical application. We firstly demonstrated strong coupling of exciton-photon with vacuum Rabi splitting up to 656 meV and low threshold polariton lasing in $CsPbBr_3$ micro/nanowires.